Eur. Phys. J. B (2012) 85: 199
DOI: 10.1140/epjb/e2012-30193-0

THE EUROPEAN PHYSICAL JOURNAL B

Regular Article

Kolmogorov turbulence, Anderson localization and KAM integrability

D.L. Shepelyansky[a]

Laboratoire de Physique Théorique du CNRS, IRSAMC, Université de Toulouse, UPS, 31062 Toulouse, France

Received 4 March 2012 / Received in final form 6 April 2012
Published online 18 June 2012 – © EDP Sciences, Società Italiana di Fisica, Springer-Verlag 2012

Abstract. The conditions for emergence of Kolmogorov turbulence, and related weak wave turbulence, in finite size systems are analyzed by analytical methods and numerical simulations of simple models. The analogy between Kolmogorov energy flow from large to small spacial scales and conductivity in disordered solid state systems is proposed. It is argued that the Anderson localization can stop such an energy flow. The effects of nonlinear wave interactions on such a localization are analyzed. The results obtained for finite size system models show the existence of an effective chaos border between the Kolmogorov-Arnold-Moser (KAM) integrability at weak nonlinearity, when energy does not flow to small scales, and developed chaos regime emerging above this border with the Kolmogorov turbulent energy flow from large to small scales.

1 Introduction

The concept of Kolmogorov turbulence 1941 [1–4] describes how the energy flows from large to small space scales in a turbulent regime. According to this concept an energy is injected on large scales, e.g. by wind, and it is absorbed on small scales due to dissipation. As a result a stationary algebraic distribution $\epsilon_k \propto k^{-5/3}$ of energy flow is established over wave modes k [1–4]. This concept was shown to be generic not only for hydrodynamic turbulence but also for other types of nonlinear waves. This phenomenon became known as the weak turbulence. With the help of diagrammatic technique Zakharov and Filonenko [5] derived the kinetic equation for weak turbulence of capillary waves and demonstrated the existence of stationary algebraic energy flows similar to those of Kolmogorov [1–3]. Later the concept of weak wave turbulence was generalized for various types of nonlinear waves as it is described in detail in [6,7]. However, an enigma of turbulence still remains as it is clearly stated in a poetic claim [8] *"Through mechanisms still only partially understood, wind transfers energy and momentum to surface water waves"*.

Indeed, the kinetic equation for energy flow from small to large wave vectors is derived in the regime of weak nonlinearity and random phase approximation [5]. A similar type of approach for wave-particle interactions is known in plasma as a quasilinear approximation [9]. This hypothesis is at the basis of the whole theory as it is directly stated by Zhakharov and Filonenko at the first paragraph of their fundamental paper [5]: *"in the theory of weak turbulence nonlinearity of waves is assumed to be small; this enables us, using the hypothesis of the random nature of the phase of individual waves, to obtain the kinetic equation for the mean square of the wave amplitudes"*. However, in finite size systems one has a a discrete spectrum of linear modes and the dynamical origins and conditions for validity of the random phase approximation and hence, for validity of the Kolmogorov concept of energy flow from small to large space scales, are still to be established.

In fact, it is known that a weak nonlinearity does not always lead to global ergodicity and chaos over all wave vectors or over all degrees of freedom. The well known example is the Fermi-Pasta-Ulam (FPU) problem [10,11] where nonlinearity should be strong enough to generate global chaos as it was pointed by Izrailev and Chirikov [12]. At present the FPU problem still remains under active studies aiming to understand its ergodic properties in the limit of low energy or weak nonlinearity [13,14]. For the FPU problem it was shown that, in the limit of very small nonlinearity combined with the resonant approximation, which is typically used for the derivation of the kinetic equation for wave [5–7], it is possible to have chaos only at small k-vectors with exponential decay of energies at high k-vectors (see [15] and Fig. 2 therein). Thus this result [15] shows that certain conditions are required for the emergence of algebraic stationary flows in the weak turbulence in finite systems.

Indeed, in the case of a few degrees of freedom it is established that in the limit of weak nonlinear perturbation almost all phase space of a typical Hamiltonian nonlinear system remains in an integrable regime known as the Kolmogorov-Arnold-Moser (KAM) integrability (see e.g. [16,17] and Refs. therein). The rigorous form of this statement is known as the KAM theory. The transition

[a] e-mail: dima@irsamc.ups-tlse.fr
http://www.quantware.ups-tlse.fr/dima

to global chaos and ergodicity requires that nonlinearity exceeds a chaos border which can be determined by numerical simulations or, in a number of cases, analytically by the Chirikov criterion [16–18]. Below the chaos border a main part of the phase space remains integrable and a chaotic spreading is possible only due to the Arnold diffusion via tiny chaotic web in a separatrix vicinity [16,17,19]. In the limit of small nonlinear perturbation the measure of these chaotic layers drops exponentially [16,17] even if for a larger number of degrees of freedom this exponential regime can become valid only at very very small perturbations [19,20].

Of course, the initial concept of Kolmogorov turbulence and weak wave turbulence considers systems of large scale with a continuous spectrum of linear waves [6,7]. However, the modern experiments on wave turbulence are done with systems of finite size (see e.g. [21–23]). Also all numerical simulations are done with the finite size systems (see e.g. [24–30]). It is recognized that in such finite systems certain resonant conditions play important role for energy flows in k-space [24,26–29]. Indeed, it is natural to assume that a discreetness of linear frequencies in a finite system can stop chaotic spreading if nonlinear frequency shifts become smaller than a typical spacing between linear resonant modes. Such a criterion has been put forward in [15] where its validity was confirmed for the FPU model in the resonant approximation.

However, the situation may be even more complicated and the energy spreading can be suppressed even in systems with everywhere dense spectrum. Indeed, in disordered systems it is known that the spreading of quantum (linear) waves can be stopped due to the phenomenon of Anderson localization [31,32] even if the spectrum of linear waves is everywhere dense and classical particles can diffusively spread over the whole system. The effects of weak nonlinearity on the Anderson localization are now under active investigations of different groups (see e.g. [33–45]). Usually the numerical simulations are done for a discrete Anderson nonlinear Shröringer equation (DANSE), which allows to perform numerical simulations in an efficient way up to very large times and thus to study wave packet spreading in space (see e.g. [36]). It is established that at moderate nonlinearity β a subdiffusive wave packet spreading continues up to enormously large times being at least by 8 orders of magnitude larger than a typical time scale in a system [33,36,40,41,43]. However, at small nonlinearity being below a certain border β_c ($\beta < \beta_c$) the spreading is absent up to maximal numerically available times. It should be pointed out that the exact mathematical results are difficult to obtain even in the limit of $\beta \to 0$ since the spectrum of the linear problem is everywhere dense so that resonances appear on large space scales [38,39]. Due to that it is difficult to develop the mathematical KAM theory in such a regime.

Below the critical value of nonlinearity $\beta < \beta_c$ the wave amplitudes decay exponentially inside a disordered layer [34,36,37,44] in a way similar to a disordered linear media in the regime of the Anderson insulator characterized by an absence of conductivity in such a system [32].

It is rather appealing to expect that the spreading in k-space of Kolmogorov turbulence will go in a way similar to the DANSE case. In fact, for the quantum Chirikov standard map, known also as the kicker rotator, it is established that for a periodic driving in time the quantum localization of dynamical chaos takes place in the momentum k-space in a way similar to the Anderson localization in a coordinate space [46–49]. The extension of this linear wave model to the case of the kicked nonlinear Schrödinger equation (KINSE) was proposed in [50]. In this KINSE model the nonlinear wave interaction takes place locally in space while we are interested in the energy spreading in the momentum k-space as it is usually the case for the weak wave turbulence [6]. In this respect the situation is different compared to the DANSE model where both nonlinear wave interaction and spreading take place in coordinate space [36]. Even if it was argued that there is a certain similarity between these two cases [33] a special more detailed analysis of the KINSE model is required. In this work the KINSE model is studied on a large time scales and the links with the DANSE model are traced in a firmer way. The implications of the obtained results for the Kolmogorov turbulence in finite size systems are discussed.

2 An example from the FPU problem

Let us discuss briefly the effects of discreteness of linear wave spectrum on example of the α-FPU problem following the results presented in [15]. It is shown there that in the long wave limit the system dynamics can be described by an effective renormalized Hamiltonian H_{RN} (see Eq. (5) in [15]):

$$H_{RN} = -\nu \sum_{k=1}^{M} k^3 J_k + 2 \sum_{k_1=1}^{M} \sum_{k_2=1}^{M-k_1} (k_1 k_2 (k_2+k_1) J_{k_1} J_{k_2} J_{k_2+k_1})^{1/2} \times \cos(\phi_{k_2+k_1} - \phi_{k_2} - \phi_{k_1}), \quad (1)$$

where J_k, ϕ_k are conjugated action-phase variable of linear k-modes, the dimensionless parameter $\nu \propto 1.5/(\sqrt{E_s} N^{3/2})$ depends on initial energy E_s, lattice size, it is inversely proportional to the nonlinear coefficient of the α-FPU model. This Hamiltonian is only a resonance approximate description of the initial FPU problem. However, it is important to see what are the properties of this Hamiltonian itself, since it has a typical form of resonant Hamiltonians considered in the theory of weak turbulence. This Hamiltonian $H_{RN} = H_{RN0} + H_{RNint}$ has an unperturbed part $H_{RN0} \propto k^3 J_k$ corresponding to the renormalized linear spectrum of long waves and a part describing the renormalized resonant interacting waves $H_{RNint} \propto \cos(\phi_{k_2+k_1} - \phi_{k_2} - \phi_{k_1})$ usually used in the theory of weak turbulence [6] (here J_k, ϕ_k are conjugated pairs of action-phase variables). It is shown in [15] that even if the dynamics of Hamiltonian H_{RN} is chaotic for

waves with $k \sim 1$ this chaos does not create energy flow to high wave vectors k and the energy density drops exponentially at large k (see Fig. 2 in [15]). This shows that the random phase approximation assumed in the weak turbulence theory can be not correct and that there can be no Kolmogorov flow from small to large wave vectors in finite size systems. Here, for us it is important to stress the properties of the renormalized Hamiltonian (1) and not of the original α-FPU model where an excitation of high k waves starts at very long times (see e.g. [13,14]). The reason for this is that the Hamilonian (1) has the usual form of wave-wave interaction Hamiltonians of the weak turbulence [6,7]. It gives a direct example that chaos on low wave vectors can be localized and isolated from integarble dynamics at high wave vectors.

3 The KINSE model description

We focus here on the KINSE model described by

$$i\hbar\frac{\partial\psi}{\partial\tau} = -\frac{1}{2}\frac{\partial^2\psi}{\partial^2 x} + \beta|\psi|^2\psi - k\cos x\psi \sum_{m=-\infty}^{\infty}\delta(\tau - mT), \tag{2}$$

where β characterizes nonlinearity, k is kick potential amplitude, T is a period between δ-function kicks periodic in time, in the following we put $\hbar = 1$. We impose the periodic boundary conditions with $\psi(x+2\pi) = \psi(x)$ and normalization condition $\int_0^{2\pi}|\psi(x)|^2dx = 1$. The linear wave expansion has the form $\psi(x) = \sum_n \psi_n \exp(-inx)/\sqrt{2\pi}$ with conserved normalization $\sum_n |\psi_n|^2 = 1$. The second moment is defined as $\sigma(t) = \sum(n-n_0)^2|\psi_n(t)|^2$, in the following we measure time t in the number of kicks (n_0 is the initial mode).

The linear model at $\beta = 0$ has been studied in a great detail (see e.g. [46–49]). The semiclassical regime of this model corresponds to $k \gg 1$, $T \ll 1$ with the classical chaos parameter $K = kT = \text{const}$. In fact K is the chaos parameter in the Chirikov standard map which describes the classical dynamics [16,17]. The classical dynamics is globally chaotic for $K > 1$ with a diffusive growth on energy proportional to σ with $\sigma = Dt$ and the diffusion rate $D \approx k^2/2$ for $K > 4$. In the quantum case this diffusion is localized due to quantum interference effects with exponentially localized Floquet states $|\psi_n| \propto \exp(-2|n-n_0|/\ell)$ and the localization length $\ell \approx D/2$ [46,47,49]. This dynamical, or Chirikov localization, is similar to the Anderson localization in disordered linear lattices where the momentum states n play the role of spacial coordinate [48,49]. In a difference from the Anderson localization, which takes place in presence of disorder, the Chirikov localization takes place in a purely dynamical system without any randomness, but due to dynamical chaos the mechanism of localization of dynamical diffusion is similar to the one of Anderson localization. In absence of kick ($K = 0$) the model is reduced to the integrable nonlinear Schödinger equation. The KINSE model has been realized experimentally with the cold atoms and Bose-Einstein condensates (BEC) in kicked optical lattices (see e.g. [51,52]). The Chirikov localization at $\beta = 0$ was observed experimentally [51], the studies of effects of BEC nonlinearity on this localization are now within experimental reach [52].

The KINSE model was introduced and studied in [50]. It was shown there that a narrow soliton has a long live time during which it follows an integrable or chaotic trajectory of the Chirikov standard map. In a regime when a soliton is destroyed it was found that there is still a suppression of classical diffusive growth of σ. In [33] it was conjectured that this growth is similar to the case of the nonlinear kicked rotator (KNR) model, where there is a nonlinear phase shift for linear modes in momentum representation (it takes place during each kick period and is proportional to $\beta|\psi_n|^2$). The evolution of the KNR model is described by a nonlinear map for the wave function [33]:

$$\bar{\psi}_n = \exp(-iT\hat{n}^2/2 - i\beta|\psi_n|^2)\exp(-ik\cos\hat{x})\psi_n. \tag{3}$$

Here the bar marks the wave function after one period of perturbation, the operator $\cos\hat{x}$ gives the Bessel coupling between the momentum states ψ_n. It was also argued [33] that the KNR behavior is similar to the case of the DANSE model, where the linear modes are also exponentially localized. The DANSE has the form

$$i\partial\psi_n/\partial\tau = E_n\psi_n + \beta|\ \psi_n\ |^2\psi_n + V(\psi_{n+1} + \psi_{n-1}), \tag{4}$$

where β characterizes nonlinearity, $V = 1$ is a hopping matrix element, on-site energies are randomly distributed in the range $-W/2 < E_n < W/2$. The spreading in this model at moderate $\beta \sim 1$ is characterized by a subdiffusive growth of the second moment σ of probability distribution:

$$\sigma(t) \propto t^\alpha \tag{5}$$

with the exponent $\alpha \approx 0.3 - 0.4$ (see details in [36,40,41]). The similar values of the spreading exponent α have been found for the KNR model [33,40,53].

If to consider the lattice sites n in (4) as the momentum states then it is clear that the nonlinear coupling in (4) is local while in the KINSE model (2) it is strongly nonlocal in momentum or k-space, as it is usual for nonlinear wave interaction in the regime of weak turbulence. Hence, the KINSE model is more adapted to the studies of the Kolmogorov turbulence in finite systems. Indeed, the kicks take place on a spacial scale of the whole system (of size 2π) and can be considered as a model of wind which pumps energy from small k-vectors (small $|n|$) to large ones. The numerical studies of the model (2) are presented in the next section.

4 Numerical results for KINSE model

To integrate numerically the evolution described by (2) it is convenient to use unitary small step integrator making small kicks in coordinate space with the local space nonlinearity and returning back and forth to the momentum space n with the fast Fourier transform as described

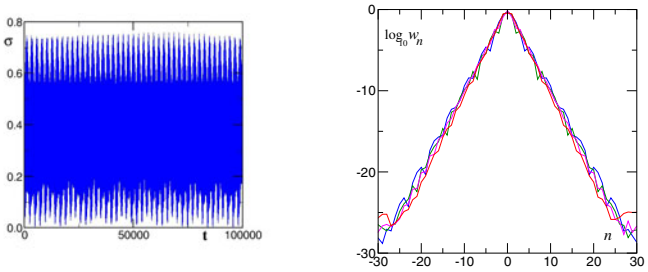

Fig. 1. (Color online) Left panel: dependence of the second moment σ on time t measured in number of kicks in (2). Right panel: probability distribution w_n over linear wave modes n at times $t = 10^3$ (blue), 10^4 (green), 10^5 (magenta), 10^6 (red) (all curves are superimposed). Here $\beta = 1$, $T = 2$, $k = 0.3$, $K = kT = 0.6$ the initial state is at zero mode $n = 0$.

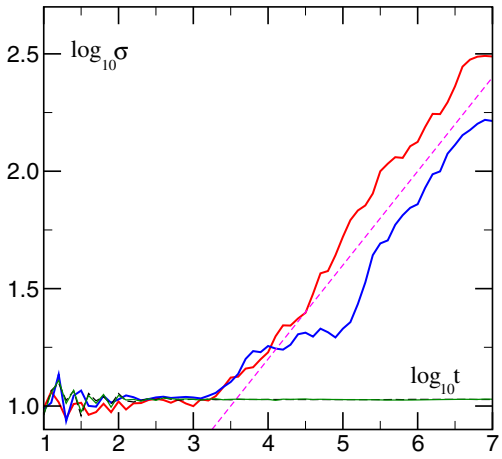

Fig. 2. (Color online) Dependence of the second moment σ of probability distribution over wave modes n on time t for (2). Here, $k = 3$, $T = 2$, $K = kT = 6$, $\beta = 0.5$ (blue curve) and $\beta = 1$ (red curve); $\sigma(t)$ is averaged over logarithmically equidistant time intervals; the initial state is $n_0 = 0$. The dashed line shows an anomalous diffusion $\sigma \sim t^\alpha$ with the exponent $\alpha = 0.4$; the fit of data in the range $3.5 \leq \log_{10} t \leq 7$ gives $\alpha = 0.346 \pm 0.014$ (for $\beta = 0.5$), $\alpha = 0.438 \pm 0.007$ (for $\beta = 1$). The horizontal dashed black curve shows data at $\beta = 0$, it practically coincides with the data for $\beta = 0.05$ shown by green curve.

in [50]. However, on very large times $t \sim 10^6$ the nonlinearity can generate exponential instability on high k-modes which is of a purely numerical origin related to discretization. To eliminate this artificial instability the simulations are done on each step in an enlarged space size (approximately 4 times larger than the size of physical modes) and after each small step the amplitudes out of the physical size are suppressed to zero. Such a method is similar to the aliasing approach [54] which efficiently suppresses numerical instability on high modes[1]. Usually the simulations are done with the total number of states $N_{tot} = 2^{10}$ and the size of physical state $N = 220$ ($-110 \leq n \leq 110$). The number of small steps N_s on one kick period varied between 100 and 1000 with a special check that it does not affect the accuracy of the results. The numerical integration method preserves the total probability up to a numerical double precision, the energy is conserved with the relative accuracy of 1% to 0.1% in absence of kicks. The similar symplectic integration method was used for the DANSE model in [36,40]. More advanced integration schemes used in [41–44] give the same results for the spreading behavior in the DANSE model. The maximal value of t reached in the present numerical simulations is $t = 10^7$.

The time evolution of the second moment $\sigma(t)$ and probability distribution over linear modes $w_n = |\psi_n|^2$ in (2) are shown in Figure 1 for the case of moderate nonlinearity $\beta = 1$ and a small kick amplitude $k = 0.3$ corresponding to the chaos parameter $K = 0.6$ being below the global chaos border $K_c \approx 1$ for the Chirikov standard map [16]. It is clear that there are only quasi-periodic oscillation of σ and that the distribution in momentum space remains exponentially localized. Thus, in this regime there is no energy flow to small scales and random phase approximation assumed in weak turbulence [5–7] is not valid. This result is similar to a usual observation that a small wind (small k here) is not able to produce a turbulent storm.

Let us now consider the regime above the classical chaos border with $K = 6$. In his regime the classical system, described by the Chirikov standard map [16], has diffusive energy growth with $\sigma \approx k^2 t/2 \approx 4t$. The results of Figure 2 at $\beta = 0$ show that this diffusion is localized by quantum interference with the localization length $\ell \approx k^2/4 \approx 2.2$ and $\sigma \sim \ell^2 \sim 10$ (the value of sigma is slightly higher than ℓ^2 due to mesoscopic fluctuations of ℓ [49]). A very weak nonlinearity $\beta = 0.05$ does not affect this localization which persists up to maximal times $t = 10^7$ reached in numerical simulations. We note that following [36] the values of σ are averaged over logarithmically equidistant time intervals that suppress fluctuations at large times.

However, at moderate nonlinearity $\beta = 0.5$ and $\beta = 1$ the second moment shows a subdiffusive growth with the algebraic exponent $\alpha \approx 0.4$. The exact fit values of α are given in the caption of Figure 2. As in [36] the statistical error bars are relatively small but there are long time correlations that can affect the real α value on large time scales as discussed in [36,40–42]. A similar value of $\alpha \approx 0.4$ has been found by Pikovsly for numerical simulations of the KINSE model by another numerical method for $t \leq 10^6$ [55]. It is interesting to note that the growth of the second moment (Fig. 2) starts at $t > 10^3$ while for DANSE it is visible at $t > 10$. A probable reason of this is a relatively smaller effective coupling between linear modes in the case of KINSE model: here the coupling is given by density fluctuations in space which have relatively smaller amplitude, compared to DANSE which has a direct coupling between modes, since kicks excite about 3–4 modes this gives a reduction of amplitude of density fluctuations in space.

The evolution of probability distribution w_n with time is shown in Figure 3 for $\beta = 0.5; 1$. It is clear that nonlinearity destroys localization: an approximately flat plateau

[1] I thank A.S. Pikovsky for a suggestion to use this aliasing method.

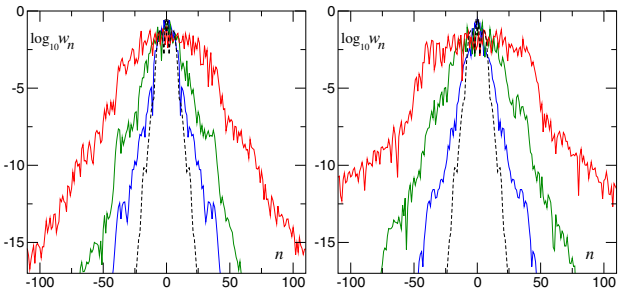

Fig. 3. (Color online) Probability distribution w_n over linear wave modes n in (2) at times $t = 10^3$ (blue), 10^5 (green), 10^7 (red) for $\beta = 0.5$ (left panel), 1 (right panel); other parameters are as in Figure 2. The dashed curve shows the probability distribution at $\beta = 0$, $t = 10^7$.

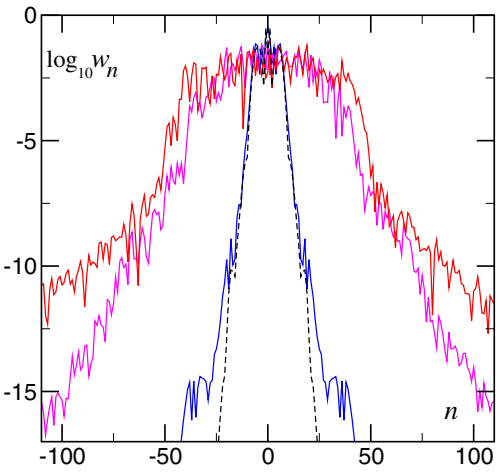

Fig. 4. (Color online) Probability distribution w_n over linear wave modes n in (2) at time 10^7 for $\beta = 0.0$ (dashed black), 0.05 (blue), 0.5 (magenta), 1 (red); other parameters are as in Figure 2.

of probability is formed ("chapeau") which size is slowly growing with time. The data for w_n at large time $t = 10^7$ show that there is a significant increase of the distribution size for $\beta = 0.5, 1$, while for $\beta = 0.05$ the probability remains localized in a way similar to the linear case $\beta = 0$. These data qualitatively confirm existence of chaos border in nonlinearity with a certain $\beta_c \sim 1/10$. However, it is not excluded that some very slow processes related to the Arnold diffusion can lead to "escape" of some small probability to larger n values at exponentially large times. Due to that reasons it is rather difficult to get an exact value of β_c and moreover, it is possible that there is a certain region of β values where the transition from one regime to another takes place. At the same time the results presented for $\beta \sim 1 > \beta_c$ and $\beta = 0.05 < \beta_c$ give a clear evinces of qualitatively different behavior above and below a certain $\beta_c \sim 1/10$.

It is interesting to note that the probability decay on the tails of the distribution (see Fig. 3) is notably slower compared to the linear case, while they were the same in the DANSE model. This is definitely related to the long range coupling between modes in the momentum space for the KINSE model. However, in spite of this long range coupling the decay on the tails remains exponential.

The results obtained for the KINSE model (2) show that the behavior of this model is qualitatively similar to the one found in the KNR (3) and DANSE (4) models: the spreading in the momentum remains localized below a certain chaos border in nonlinearity strength, while above this border the spreading continues in a subdiffusive way with the algebraic exponent being close to the value $\alpha \approx 0.4$ found previously for KNR and DANSE. The main difference from DANSE is that for KINSE we have interchange between momentum and coordinate spaces. However, such a similarity between momentum and coordinate space is well known [48,49] and was already discussed for the KNR model in [33]. The main new aspect of the KINSE model is a long range coupling in the momentum space due to the locality of wave interaction in the coordinate space. However, due to a localized nature of linear eigenmodes in the momentum space this long range coupling still can give transitions only on a size of localization length ℓ and this does not produce a qualitative difference from the case of short range integration appearing in DANSE. A similar situation appears for the model of two particles with Coulomb interaction in the regime of Anderson localization as it is discussed in [56].

One of the features of the KINSE model is its integrability in absence of kicks, since it is reduced to the nonlinear Schrödinger equation. However, the presence of kicks generates chaos of classical rays and due to this the above integrability becomes unimportant. Indeed, we see that KINSE shows the behavior similar to DANSE and KNR models, and with the KNR model with random rotating energies (see [53]). All the above models have a generic type on linear modes spectrum, known as a pure point spectrum in the field of Anderson localization. Due to that a generic nonlinear perturbation of this spectrum is expected to generate a generic behavior that is indeed confirmed by the results presented here and in works on other models.

5 Kolmogorov turbulence in Sinai billiard

On a first glace one can get an impression that the KINSE model is a rather specific one: it is one-dimensional, there are kicks etc. However, it is known that the Chirikov standard map is generic and describes a variety of real physical systems [16,17]. Also it is known that the Chirikov localization found first in the linear KINSE and NKR models at $\beta = 0$ appears in a variety of real systems (see e.g. [57,58]). Thus we expect that the behavior found here for the KINSE model at finite nonlinearity β will appear in more realistic systems.

Let us discuss an example of such a system. For that we consider the nonlinear Schödinger equation in a two-dimensional chaotic billiard (e.g. the Sinai billiard [59]) in a presence of a monochromatic driving:

$$i\partial\psi/\partial\tau = -\Delta\psi/2 + V(x,y)\psi + \beta|\psi|^2\psi + F\sin(\omega\tau)x\psi. \quad (6)$$

Here Δ is 2D Laplace operator, the potential $V(x, y)$ is determined by a rigid boundary of the billiard, F and ω are the amplitude and frequency of a monochromatic force acting on a particle inside the chaotic billiard. We assume that the classical dynamics inside the billiard is chaotic that leads to quantum chaos and ergodicity of the eigenstates of the linear problem (see e.g. [60]). The microwave monochromatic force acting on a classical particle creates a diffusive growth of its energy with time but the quantum interference effects lead to exponential localization of this diffusion (at $\beta = 0$) [61], in a way similar to the KINSE and KNR models at $\beta = 0$. It is interesting to know how the nonlinear term with β in (6) will affect this localization and if nonlinearity can create the Kolmogorov flow of energy from small to large wave vectors. An analogy with the models of the previous sections gives an idea that at weak F and β there will be no energy flow to high level numbers of the linear quantum billiard. However, for the quantum billiard there is a new element which we discuss below.

Indeed, the density of energy levels inside the 2D quantum billiard is approximately constant, up to quantum fluctuations [60]. Due to that the energies of quantum levels grow with the level number n, approximately as $E_n \sim \rho n$ where ρ is the average density of levels. Such a behavior of energy levels is different from the case of DANSE where all unperturbed energy levels are located inside a finite energy band. A linear growth of E_n with n corresponds to a presence of a static Stark field with an additional term $\delta E_n = fn$. Such a DANSE model with a Stark field has been studied in [62] and it was shown that a subdiffusive spreading goes in a way similar to the DANSE model at moderate values of f. However, for a billiard there is a minimal energy so that we have only $n \geq 0$ (like a triangular potential). To model such a situation one needs to assume that in the DANSE model (4) there is an additional energy shift $\delta E_n = f|n|$. Thus the DANSE model with such a modulus Stark term reproduces the energy growth with level number typical of the quantum billiard. We will call this the Stark DANSE model of billiard (SDANSEBIL model). The numerical simulations of this SDANSEBIL can be done in the same rather efficient way as it is described in [62]. The comparison of the results at moderate nonlinearity $\beta = 1$ for $f = 0$ (DANSE) and $f = 0.5$ (SDANSEBIL) is presented in Figures 5 and 6. It shows that a finite f reduces the value of σ almost by two orders of magnitude and that the probability distribution over levels is localized in a much stronger way compared to the case with $f = 0$. The physical origin of this suppression should be attributed to the energy conservation which for $f > 0$ leads to a more rapid decrease of probability on high levels: for a homogeneous probability distribution on levels $0 \leq n \leq n_{max}$ the energy conservation imposes $|\psi_{n_{max}}|^2 \sim 1/(fn_{max}^2)$ while at $f = 0$ the restriction from norm conservation gives slower decay of probability with $|\psi_{n_{max}}|^2 \sim 1/n_{max}$. Due to this reason the spearing over levels is suppressed stronger in the presence of finite static field f and triangular form of energies $\delta E_n \propto |n|$. We note that the case with $\delta E_n \propto n$, considered in [62], does not give additional restrictions due to cancellations of negative and positive n contributions. The obtained results show that the transition to ergodicity in the SDANSEBIL model is practically absent and thus there is no energy flow to high wave vectors.

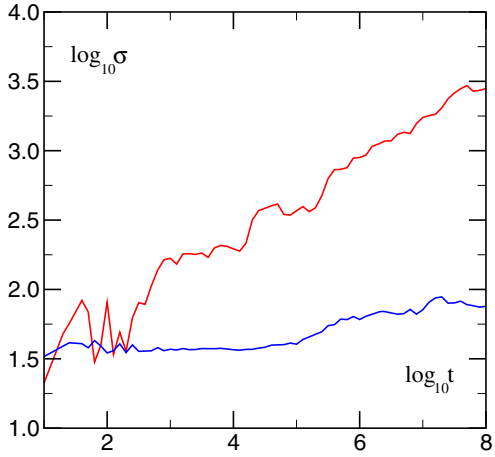

Fig. 5. (Color online) Dependence of the second moment σ in the DANSE model (4) at $W = 4$, $V = 1$, $\beta = 1$ (red curve) and in the DANSE model with additional static field potential (SDANSBIL model)) with $\delta E_n = f|n|$ at $f = 0.5$ (blue curve) at the above parameters and the same disorder realization. The initial state is at $n = 0$.

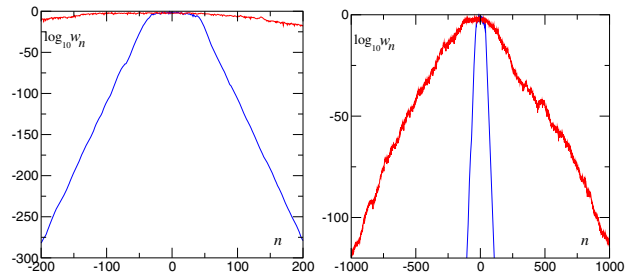

Fig. 6. (Color online) Probability distribution w_n over linear wave modes n at times 10^8 for the two cases of Figure 5 with the same attribution of colors; two panels show the same data on different scale.

It should be noted that the numerical results presented in this section are done for SDANSEBIL model described in the previous paragraph. It is argued that this model captures the main features of the more physical initial model of equation (6). Some arguments related to the density of energy levels are give above. There are however certain differences between two models, e.g. the energy is conserved in SDANSEBIL but not in equation (6). However, the DANSE and KINSE models have the same type of difference and still they show the similar behavior. Thus, due to similarity between DANSE and KINSE and KNR models discussed in previous sections we make a conjecture that the behavior similar to the one found for SDANSEBIl model will take place for the evolution in the nonlinear billiard model (6). As a results of that observation it is possible to make a conjecture that there will be no energy flow to high wave vectors for the Kolmogorov turbulence in Sinai billiard described by equation (6). Of course, it would be very interesting to perform direct numerical

simulations of the model (6) but this would require much more advanced and heavy numerical simulations.

6 Discussion

In this work we discussed the properties of weak wave turbulence in finite systems. On the basis of numerical simulations and analytical results we argue that the discrete spectrum of linear frequencies, typical for finite systems, imposes specific conditions for appearance of the Kolmogorov energy flow from large to small spacial scales. In absence of random phase approximation such a flow can appear only above a chaos border at a sufficiently large nonlinear coupling between linear modes and/or strong driving force. The considered models show that the Anderson localization, appearing in the wave vector space of linear modes, can stop the energy flow from large to small scales if nonlinearity is below the chaos border and the system is in the regime of KAM integrability. A similar situation appears at a small amplitude of energy pumping. In a qualitative way such a regime corresponds to a small wind which cannot generate turbulent ocean waves. Of course, the models analyzed here are relatively simple and hence, the numerical and experimental studies of more realistic systems, like e.g. the model (6), are highly desirable. Such studies will allow to understand a new regime of nonlinear waves where interplay between Anderson localization, nonlinearity, KAM integrability and Kolmogorov turbulence in finite systems opens new interesting and unsolved questions.

Finally, it is useful to note that a quasiperiodic driving of the KINSE model at $\beta = 0$ with two incommensurate frequencies can create the Anderson transition with appearance of energy flow to high momentum states [63,64]. Such a transition has been observed recently in experiments with cold atoms in kicked optical lattices [65]. Thus it is possible that a transition to weak turbulence in finite systems is somewhat similar to the Anderson transition in disordered solids. In such a scenario the regime of Anderson insulator corresponds to laminary waves and absence of energy flow from small wave vectors to large ones, while the metallic phase allows to have a turbulent energy flow from small to larger wave vectors. The analysis of possible links between these phenomena requires further investigations. The modern techniques of ultra cold atoms and BEC (see e.g. [51,52,65]) allow to study experimentally the effects of nonlinear wave interactions in such systems.

I thank A.S. Pikovsky for stimulating discussions and critical remarks.

References

1. A.N. Kolmogorov, Dokl. Akad. Nauk SSSR **30**, 299 (1941)
2. A.N. Kolmogorov, Dokl. Akad. Nauk SSSR **32**, 19 (1941) (in Russian) (English trans. Proc. R. Soc. Ser. A **434**, 19 (1991))
3. A.N. Kolmogorov, Dokl. Akad. Nauk SSSR **434**, 15 (1991)
4. A.M. Obukhov, Izv. AN SSSR Ser. Geogr. Geofiz. **5**, 453 (1941) (in Russian)
5. V.E. Zakharov, N.N. Filonenko, J. Appl. Mech. Tech. Phys. **8**, 37 (1967)
6. V.E. Zhakharov, V.S. L'vov, G. Falkovich, *Kolmogorov Spectra of Turbulence* (Springer-Verlag, Berlin, 1992)
7. S. Nazarenko, *Wave Turbulence* (Springer-Verlag, Berlin 2011)
8. A.C. Newell, V.E. Zhakharov, Phys. Rev. Lett. **69**, 1149 (1992)
9. A.A. Vedenov, E.P. Velikhov, R.Z. Sagdeev, Nucl. Fus. **1**, 82 (1961)
10. E. Fermi, J. Pasta, S. Ulam, M. Tsingou, *Studies of nonlinear problems. I*, Los Alamos Report No. LA-1940, 1955 (unpublished)
11. E. Fermi, *Collected Papers* (University of Chicago Press, Chicago, 1965), Vol. 2, p. 978
12. F.M. Izrailev, B.V. Chirikov, Dokl. Akad. Nauk SSSR **166**, 57 (1988) (in Russian) (English trans. Sov. Phys. Doklady **11**, 30 (1966))
13. The Fermi-Pasta-Ulam problem, in *Springer Lecture Notes in Physics*, edited by G. Gallavotti (2008), Vol. 728
14. G. Benettin, R. Livi, A. Ponno, J. Stat. Phys. **135**, 873 (2009)
15. D.L. Shepelyansky, Nonlinearity **10**, 1331 (1997)
16. B.V. Chirikov, Phys. Rep. **52**, 263 (1979)
17. A.J. Lichtenberg, M.A. Lieberman, *Regular and Chaotic Dynamics* (Springer, Berlin, 1992)
18. D. Shepelyansky, Scholarpedia **4**, 8567 (2009)
19. B.V. Chirikov, V.V. Vecheslavov, Sov. Phys. JETP **85**, 616 (1997) [Zh. Eksp. Teor. Fiz. **112**, 1132 (1997)]
20. M. Mulansky, K. Ahnert, A. Pikovsky, D.L. Shepelyansky, J. Stat. Phys. **145**, 1256 (2011)
21. S. Lukaschuk, S. Nazarenko, S. McLelland, P. Denissenko, Phys. Rev. Lett. **103**, 044501 (2009)
22. D. Snouck, M.-T. Westa, W. van de Water, Phys. Fluids **21**, 025102 (2009)
23. P.J. Cobelli, V. Pagneux, A. Maurel, P. Petitjeans, J. Fluid Mech. **666**, 445 (2011)
24. Y.V. Lvov, S. Nazarenko, B. Pokorni, Physica D **218**, 24 (2006)
25. S. Nazarenko, M. Onorato, Physica D **219**, 1 (2006)
26. E. Kartashova, Phys. Rev. Lett. **98**, 214502 (2007)
27. E. Kartashova, S. Nazarenko, O. Rudenko, Phys. Rev. E **78**, 016304 (2008)
28. D. Proment, S. Nazarenko, M. Onorato, Phys. Rev. A **80**, R056103 (2009)
29. E. Kartashova, Europhys. Lett. **87**, 44001 (2009)
30. N. Sasa, T. Kano, M. Machida, V.S. Lâvov, O. Rudenko, M. Tsubota, Phys. Rev. B **84**, 054525 (2011)
31. P.W. Anderson, Phys. Rev. **109**, 1492 (1958)
32. E. Akkermans, G. Montambaux, *Mesoscopic Physics of Electrons and Photons* (Cambridge University Press, Cambridge, 2007)
33. D.L. Shepelyansky, Phys. Rev. Lett. **70**, 1787 (1993)
34. D.L. Shepelyansky, Physica D **86**, 45 (1995)
35. M.I. Molina, Phys. Rev. B **58**, 12547 (1998)
36. A.S. Pikovsky, D.L. Shepelyansky, Phys. Rev. Lett. **100**, 094101 (2008)
37. S. Tietsche, A. Pikovsky, Europhys. Lett. **84**, 10006 (2008)
38. J. Bourgain, W.-M. Wang, J. Eur. Math. Soc. **10**, 1 (2008)

39. S. Fishman, Y. Krivolapov, A. Soffer, in Nonlinearity arXiv:1108.2956 (2011)
40. I. Garcia-Mata, D.L. Shepelyansky, Eur. Phys. J. B **71**, 121 (2009)
41. S. Flach, D.O. Krimer, C. Skokos, Phys. Rev. Lett. **102**, 024101 (2009)
42. T.V. Laptyeva, J.D. Bodyfelt, D.O. Krimer, Ch. Skokos, S. Flach, Europhys. Lett. **91**, 30001 (2010)
43. M. Mulansky, A. Pikovsky, Europhys. Lett. **90**, 10015 (2010)
44. M. Johansson, G. Kopidakis, S. Aubry, Europhys. Lett. **91**, 50001 (2010)
45. A. Pikovsky, S. Fishman, Phys. Rev. E **83**, 025201 (2011)
46. B.V. Chirikov, F.M. Izrailev, D.L. Shepelyansky, Sov. Scient. Rev. C **2**, 209 (1981) [Sec. Math. Phys. Rev.], Harwood Acad. Publ., Chur, Switzerland
47. B.V. Chirikov, F.M. Izrailev, D.L. Shepelyansky, Physica D **33**, 77 (1988)
48. S. Fishman, D.R. Grempel, R.E. Prange, Phys. Rev. Lett. **49**, 509 (1982)
49. D.L. Shepelyansky, Physica D **28**, 103 (1987)
50. F. Benvenuto, G. Casati, A.S. Pikovsky, D.L. Shepelyansky, Phys. Rev. A **44**, R3423 (1991)
51. M. Raizen, D.A. Steck, Scholarpedia **6**, 10468 (2011)
52. A. Ullah, M.D. Hoogerland, Phys. Rev. E **83**, 046218 (2011)
53. G. Gligoric, J.D. Bodyfelt, S. Flach, Europhys. Lett. **96**, 30004 (2011)
54. Wikipedia contributors, *Aliasing* (Wikipedia, The Free Encyclopedia, 2012)
55. A.S. Pikovsky, private comminication, 2011
56. D.L. Shepelyansky, Phys. Rev. B **61**, 4588 (2000)
57. S. Fishman, Scholarpedia **5**, 9816 (2010)
58. D. Shepelyansky, Scholarpedia **7**, 9795 (2012)
59. I.P. Kornfeld, S.V. Fomin, Ya.G. Sinai, *Ergodic Theory* (Springer, New York, 1982)
60. H.-J. Stöckmann, Scholarpedia **5**, 10243 (2010)
61. T. Prosen, D.L. Shepelyansky, Eur. Phys. J. B **46**, 515 (2005)
62. I. Garcia-Mata, D.L. Shepelyansky, Eur. Phys. J. B **71**, 121 (2009)
63. F. Borgonovi, D.L. Shepelyansky, J. Phys. I **6**, 287 (1996)
64. D.L. Shepelyansky, *Anderson transition in three and four effective dimensions for the frequency modulated kicked rotator* (2011), arXiv:1102.4450
65. J. Chabe, G. Lemarie, B. Gremaud, D. Delande, P. Szriftgiser, J.C. Garreau, Phys. Rev. Lett. **101**, 255702 (2008)